In situ synchrotron X-ray studies of dense thin-film strontium-doped lanthanum manganite solid oxide fuel cell cathodes

Kee-Chul Chang[1], Brian Ingram[2], Balasubramaniam Kavaipatti[3], Bilge Yildiz[4], Daniel Hennessy[1], Paul Salvador[3], Nadia Leyarovska[5] and Hoydoo You[1]

[1]Materials Science Division, Argonne National Laboratory, 9700 S Cass Ave., Argonne, IL 60439, U.S.A

[2]Chemical Sciences and Engineering Division, Argonne National Laboratory, 9700 S Cass Ave., Argonne, IL 60439, U.S.A

[3]Department of Materials Science and Engineering, Carnegie Mellon University, 5000 Forbes Ave., Pittsburgh, PA 15213, U.S.A

[4]Department of Nuclear Science and Engineering, Massachusetts Institute of Technology, 77 Massachusetts Ave., Cambridge, MA 02139, U.S.A

[5]X-ray Science Divison, Advanced Photon Source, Argonne National Laboratory, 9700 S Cass Ave., Argonne, IL 60439, U.S.A

ABSTRACT

Using a model cathode-electrolyte system composed of epitaxial thin-films of $La_{1-x}Sr_xMnO_{3-\delta}$ (LSM) on single crystal yttria-stabilized zirconia (YSZ), we investigated changes of the cation concentration profile in the LSM during heating and under applied potential using grazing incidence x-rays. Pulsed laser deposition (PLD) was used to grow epitaxial LSM(011) on YSZ(111). At room temperature, we find that Sr segregates to form Sr enriched nanoparticles. When the sample heated to 700°C, Sr is slowly reincorporated into the film. We also find different amounts of Sr segregation as the X-ray beam is moved across the sample. The variation in the amount of Sr segregation is greater on the sample that has been subject to 72 hours of applied potential, suggesting that the electrochemistry plays a role in the Sr segregation.

INTRODUCTION

The solid oxide fuel cell (SOFC) has advantages of high efficiency and fuel-flexibility but is not yet economically competitive enough to gain widespread acceptance. Between the cathode, anode and electrolyte of SOFC, it is well known that the cathode resistance dominates the overall cell resistance and hence has the most room for improvement. Therefore, efforts to improve SOFC performance have been focused on the cathode but a more fundamental understanding of the mechanism and kinetics of the oxygen reduction reaction at the cathode is still lacking.

We investigate a model system of pulsed laser deposited LSM on a single crystal YSZ electrolyte. Although LSM is widely used as cathodes for industrial SOFC in a porous form, such electrodes has complex electrochemical reaction pathways with no easy means for site specific X-ray characterization. Our model system was chosen to simplify reaction pathways as well as making the electrode amendable to grazing incidence X-ray characterization techniques.

This paper focuses on the question of cation motion inside the cathode under long term applied potential. For perovskite LSM, defect thermodynamic models [1,2], based on precision balance weight measurements on a powder sample subject to certain temperature and oxygen

partial pressure [3,4], predict that the oxygen is superstoichiometric due to cation vacancies at atmospheric oxygen pressure. Decrease in oxygen partial pressure, which is thermodynamically equivalent to cathodic applied potential, is needed for ABO_3 perovskite stoichiometry and further decrease is needed to induce oxygen vacancies. Higher temperatures also drive oxygen toward stoichiometry.

As a consequence, gradients in oxygen chemical potential in the electrode under applied potential can induce kinetic demixing of cations in the transition metal oxide. There have been previous studies [5,6] on LSM which suggests Sr segregates to the surface and the effect of such segregation is to deter cathode performance [7]. This paper aims to study this phenomenon using in-situ X-ray techniques.

EXPERIMENT

Pulsed laser deposition (PLD) was used to grow 60nm thick LSM films on a single crystal YSZ(111) substrate at 750°C in 50mTorr O_2. The samples were cooled to room temperature in 300 mTorr O_2. X-ray diffraction measurements showed that the LSM grew epitaxially in the (011) orientation with 6-fold domains on the YSZ. Note that the (011) planes are highly polar for perovskite, with alternating +4 and -4 layers.

We prepared electrical contacts on the samples for in situ electrochemical measurements by fixing Pt mesh on the backside of the YSZ crystal and Pt wires on the LSM surface with Pt paste as illustrated in figure 1a. The LSM also had a thin middle wire, consisting of a 50 μm thick Pt wire fixed on place with Pt ink to insure that the area activated by the applied potential will be evenly distributed on the surface. The electrochemical measurements were done using a Princeton Applied Research 273A potentiostat.

Our experiments were preformed in beamline 12BM at the Advanced Photon Source. The electrochemical cell was fixed on an alumina tube and the system was mounted on a 6 circle diffractometer. We used an infrared spot heater (Research Inc.) to heat the sample to the desired temperature and a Vortex detector (Radiant Technologies) to measure the X-ray fluorescence from the sample for spectroscopy. In the current setup, we cannot control the oxygen pressure and the experiment was done in air.

We use Total Reflection X-ray Fluorescence (TXRF) to depth profile the LSM film. The index of refraction for X-rays in matter is less than 1, which implies that there is total external reflection of X-rays below the critical angle;

$$\alpha_c \approx \lambda \sqrt{\frac{\rho r_0}{\pi}} \qquad (1)$$

where λ is the X-ray wavelength, ρ is the electron density of the material and r_0 is the classical electron radius. Below the critical angle, the X-ray weakly penetrate into the sample via an exponentially decaying evanescent wave and the interference between the incident and reflected X-rays sets up large electric fields above the surface. By controlling the X-ray incidence angle, we can confine the penetration of the X-rays inside the perovskite film to its surface region as illustrated in figure 1b. By setting the X-ray energy above the absorption edges of all the elements of interest inside the film, we can collect the X-ray fluorescence as a function of X-ray incidence angle to depth profile the composition of the film. It should be noted that using

grazing incidence imposes the restriction that the sample surface be flat, although some degree of small scale roughness can be modeled in the data analysis.
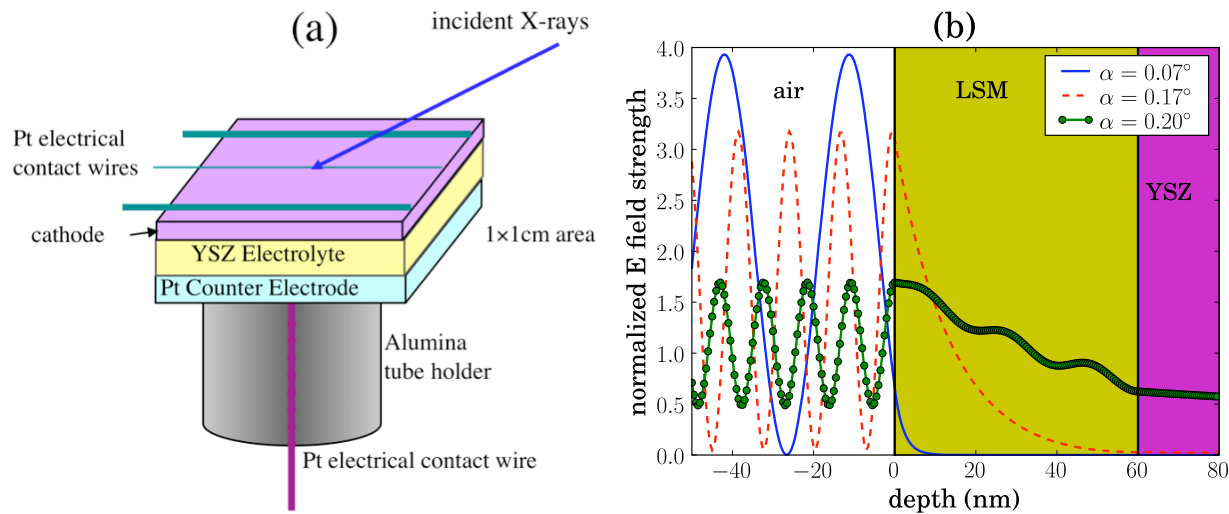

Figure 1 (a) Schematic diagram of the in-situ electrochemical X-ray cell (b) Illustration of the effect of different incidence angles on the X-ray electrical fields inside the sample.

DISCUSSION

The TXRF of 60nm thick $La_{0.7}Sr_{0.3}MnO_3$ on YSZ(111) under different conditions is shown in figure 2a. The X-ray beam was positioned slightly away from the middle wire. At room temperature, Sr fluorescence is enhanced below the critical angle (denoted by a dotted vertical line). This increase is most likely caused by nanoparticles which are not a part of the LSM surface. Such particles will be subject to higher electric fields due to the interference between incident and reflected X-rays. Atomic force microscopy subsequently revealed that there are 10-40nm high particles covering the surface of the LSM at room temperature (not shown) as expected.
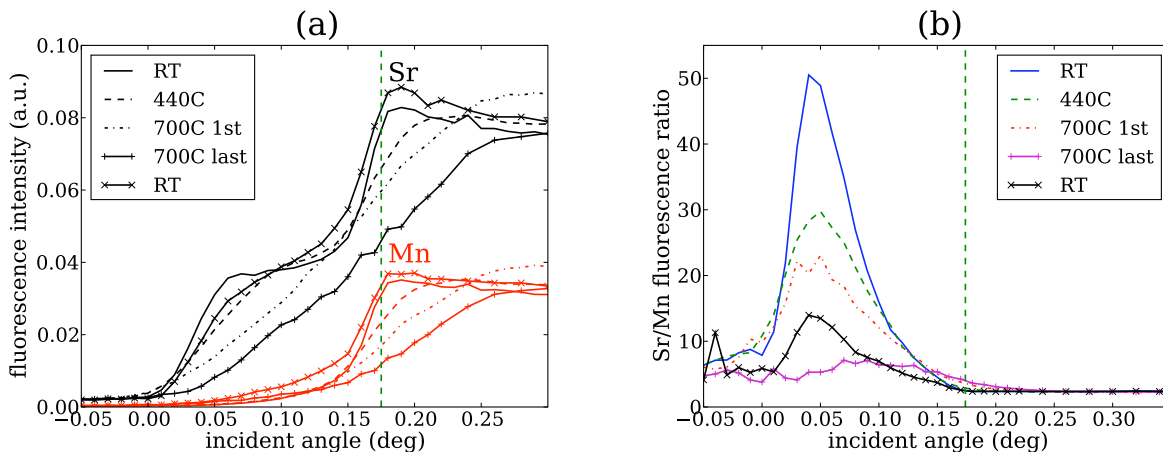

Figure 2. (a) TXRF of $La_{0.7}Sr_{0.3}MnO_3$. '700°C 1st' denotes the scan taken before electrochemistry while '700°C last' denote a scan taken after applying between -135mA and +100mA of current. The time elapsed between the two 700°C scans is around 16 hours (b) Sr/Mn fluorescence ratio shows the relative level of Sr enrichment compared with Mn.

Heating the sample slowly removes the Sr segregation which can be seen more clearly in terms of Sr/Mn ratio in figure 2b. The sample may also undergo warping at high temperature which causes the critical angle to be smeared out, but comparing the scans at 700°C shows that there is a definite trend toward Sr incorporation into the LSM electrode.

On a second set of 60nm thick $La_{0.8}Sr_{0.2}MnO_3$ on YSZ(111), one sample was annealed to 800°C for 1 hour to sinter the Pt middle wire to the surface, while a second sample with the middle wire was conditioned with -280mV applied potential at 800°C for 72 hours. We then moved the 1mm wide X-ray across the sample in 1mm steps, starting from one edge with a thick Pt pad. Since the YSZ substrate is 1x1cm in dimension and the Pt pads were about 0.5mm wide, we only needed about 8 steps to reach the other side of the sample. La, Mn and Sr fluorescence were each normalized to the above critical angle region and plotted in figure 3. In figure 3a, we can see that the level of Sr segregation is fairly uniform across all the different beam positions, while in figure 3b the Sr segregation levels vary widely.
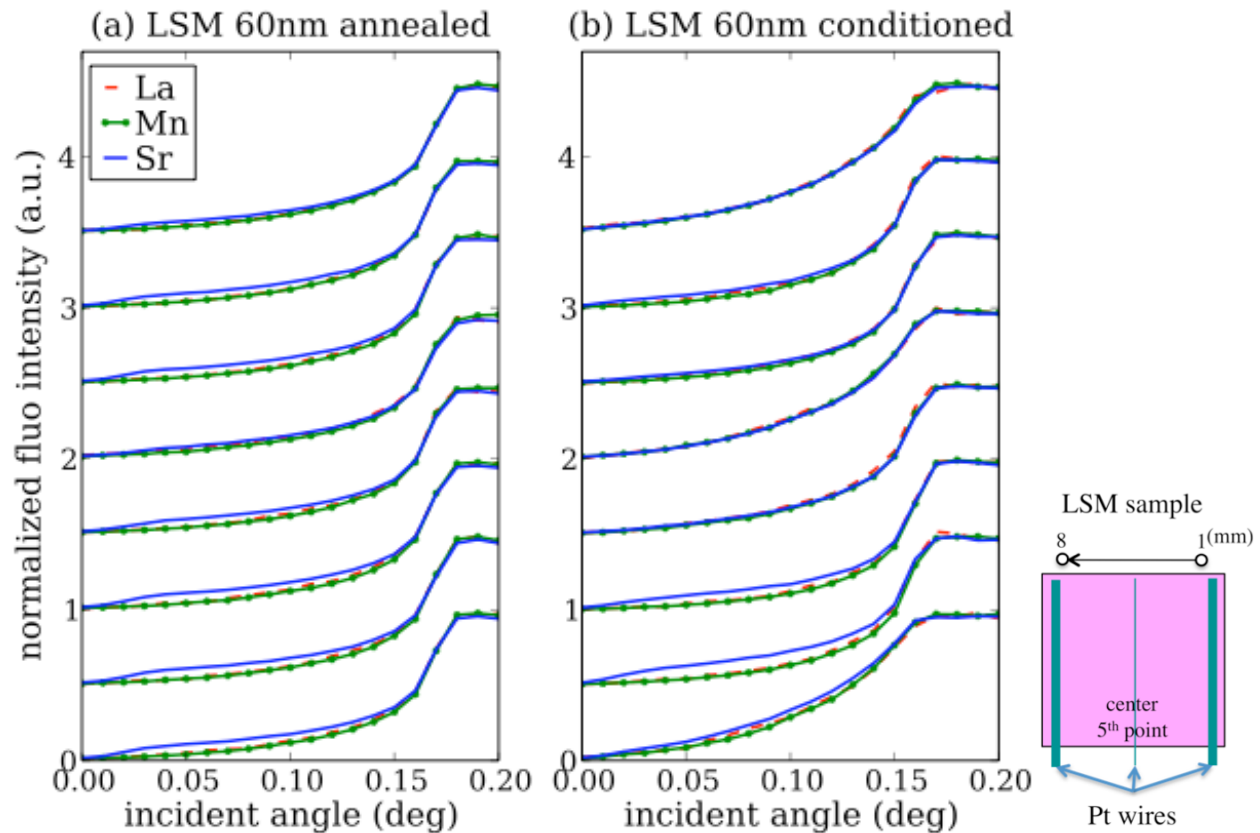

Figure 3. Position dependent TXRF of (a) LSM annealed at 800°C for 1 hour (b) LSM heated to 800°C and conditioned with -280mV applied potential. Each scan is offset by 0.5 for clarity

This can be seen more clearly by taking the average Sr/Mn ratio below the critical angle as shown in figure 4a. For the conditioned sample, a finer resolution data with 0.2mm beam width and 0.25mm step size was taken and overlaid on the 1mm beamwidth data. Both data shows that the conditioned sample has a highly Sr segregated region in between the middle Pt wire and the side Pt pad. The annealed LSM sample has a much flatter Sr/Mn ratio variation, with only a sharp dip near the middle wire position.

The Sr/Mn ratio can be contrasted with the La/Mn ratio shown in figure 4b. In the La/Mn case, there is hardly variation with position. One notable exception is at the middle wire position, where the annealed LSM has more La on the surface compared with Mn, where as the conditioned LSM seems to have less La.
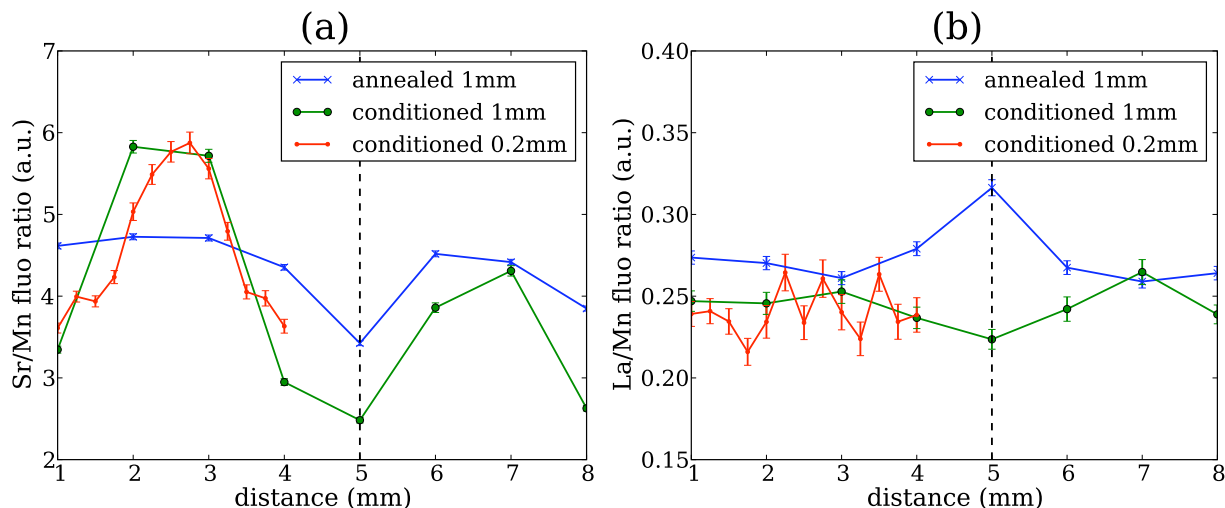

Figure 4. Below critical angle averaged (a) Sr/Mn and (b) La/Mn fluorescence ratio

These position dependent TXRF results suggest that the amount of cation segregation is a function of electrochemical activity. The drop in Sr segregation at the middle wire may be due to the surface damage caused by the Pt ink used to fix the middle wire in place. We also looked at the fluorescence of Pt to see whether the diffusion of Pt may contribute to the cation segregation but we measured similar amounts of Pt away from the Pt wire or pads. In separate electrochemical measurements, we determined that about 70% of the sample surface is active while potential is applied, which translates to areas about 1mm away from the wires. The areas of maximum Sr segregation correlate well to the inactive areas during conditioning.

CONCLUSIONS

Using grazing incidence X-rays in TXRF, we found evidence of Sr segregation into Sr enriched nanoparticles for LSM(011) films on YSZ(111). Sr segregation reappears upon heating and cooling, showing that it is a thermodynamically stable state at this temperature. Annealed LSM sample displayed almost uniform Sr segregation over the surface, while the conditioned LSM had greater variation in the Sr segregation level.

In the future, we will focus on characterizing different areas on the LSM surface, as well as preparing samples with different Pt wire spacing.

ACKNOWLEDGMENTS

REFERENCES

1. D.S. Mebane, Y.J. Liu, and M.L. Liu, Solid State Ionics **178**, 1950 (2008).
2. F.W. Poulsen, Solid State Ionics **129**, 145 (2000).
3. J. Mizusaki, H. Tagawa, K. Naraya, and T. Sasamoto, Solid State Ionics **49**, 111 (1991).
4. J.H. Kuo, H.U. Anderson, and D.M. Sparlin, J. Solid State Chem. **83**, 52 (1989).
5. N. Caillol, M Pijolat, and E. Siebert, Appl. Surf. Sci. **253**, 4641 (2007).
6. H. Dulli, P.A. Dowben, S.H. Liou, and E.W. Plummer, Phys. Rev. B **62**, R14629 (2000).
7. S.P. Jiang, and J.G. Love, Solid State Ionics **138**, 183 (2001).